Available online at www.sciencedirect.com
SCIENCE DIRECT
Journal of Molecular Catalysis A: Chemical 249 (2006) 149–157
JOURNAL OF MOLECULAR CATALYSIS A: CHEMICAL
www.elsevier.com/locate/molcata

Kinetic modeling of the methylcyclohexane transformation over H-USY: Deactivating effect of coke and nitrogen basic compounds

G. Caeiro [a,b], P. Magnoux [b], J.M. Lopes [a], F. Lemos [a], F. Ramôa Ribeiro [a,*]

[a] *Centro de Engenharia Biológica e Química, Instituto Superior Técnico, Av. Rovisco Pais, 1049-001 Lisbon, Portugal*
[b] *Laboratoire de Catalyse en Chimie Organique, Chimie 7A-3, 40 Avenue du Recteur Pineau, 86022 Poitiers Cedex, France*

Received 8 November 2005; received in revised form 5 January 2006; accepted 5 January 2006
Available online 13 February 2006

Abstract

In this paper, a transient pseudo-homogeneous model was developed with the objective of describing the activity, product distribution and deactivation with time on stream for the methylcyclohexane transformation over H-USY at 350 °C. The reaction scheme details the reactant, cyclopentane ring isomers, alkenes, alkanes, aromatics and coke. The existence of adsorbed species is neglected, exception made for coke molecules that remain trapped inside the catalyst, being responsible by the catalyst deactivation. The effect of a model basic nitrogen molecule (quinoline) in the feed is also described by the model; both its roles as a poison and as coke precursor are accounted for. The fitting was done using data determined experimentally at 350 °C for 1/WHSV (weight hourly space velocity) values of 12 and 4 min, as a function of time on stream. The model fits extremely well the activity, deactivation and product distribution, coke included.

Keywords: H-USY zeolite; Methylcyclohexane; Quinoline; Coke; Kinetic modeling

1. Introduction

Fluid catalytic cracking (FCC) is one of the key processes in a modern refinery [1]. Important amounts of gasoline and light olefins are produced in this process. It is one of the most important industrial processes worldwide and, as a consequence, even minor improvements in conversion and selectivities will have a very significant economical impact. These enhancements can be obtained at various levels, namely the design of more efficient catalysts and a better control of the process.

Currently, the FCC catalyst main active component is the H-USY zeolite, it can be obtained by hydrothermal treatment (steaming) of the Y zeolite structure. Acid zeolites, like H-USY, are strongly deactivated during cracking reactions [2–12], mainly due to the formation of polyaromatic compounds known as coke. Coke formation has a strong impact on the performance of the catalyst, modifying the conversion and products selectivity, besides playing an important role in the heat balance of the FCC unit. This fully justifies the efforts on developing fundamental and systematic kinetic models accounting for coke formation. The presence of poisons in the feed is also a critical matter; due to the decrease in acid sites resulting from the steaming treatment, the H-USY zeolite is particularly sensitive to the presence of basic poisons in the feed.

Several feedstocks can be used in the FCC process, and one of the most common is the vacuum gas oil (VGO) produced in the crude oil vacuum distillation. It is composed mainly by naphtenes, aromatics and alkanes. Contrarily to alkanes and aromatics, not much can be found in literature regarding the catalytic cracking of naphtenes over H–Y zeolites [13–18]. The study of this transformation is particularly interesting because it allows a better understanding of the mechanisms of formation of aromatics and coke. The cracking chemistry of naphtenes is very complex due to the high number of reactions that can occur simultaneously: ring opening, hydrogen transfer, isomerization, secondary cracking and coke formation.

Apart from hydrocarbons, FCC feeds contain non-negligible amounts of metals: Fe, Ni, V (0–200 ppm), oxygen (0–2%), sulphur (0–7.5%) and nitrogen (0–1700 ppm). About 25–30% of this nitrogen (400–600 ppm) is contained in basic compounds: pyridine, quinoline, isoquinoline, acridine and phenanthridine

* Corresponding author. Tel.: +351 21 841 9073; fax: +351 21 841 9198.
E-mail address: qramoa@ist.utl.pt (F.R. Ribeiro).

1381-1169/$ – see front matter © 2006 Elsevier B.V. All rights reserved.
doi:10.1016/j.molcata.2006.01.011

or alkyl derivates of theses compounds. The others are not basic and usually include a pyrrol nucleus: pyrrol, indole and carbazole.

Currently, it is commonly accepted that two cracking mechanisms can occur: protolytic (monomolecular) [19–21] and β-scission (bimolecular) [22–24]. The relative importance of each one depends on the reaction temperature and catalyst properties. Modeling the cracking reaction network is an extremely complex task [18,25–42]; there are several reactions that occur simultaneously, the number of species present in the reactor is extremely high and the acidity of the sites present in the zeolite is often non-uniform [42]. Even in a catalytic test unit, as the one used in this work, with only one reactant and one poison, the number of possible reactions and species contribute, to a great extent, to the difficulty in the construction of a complete model. In order to overcome the difficulties of dealing with detailed models, a variety of approaches can be used. Normally, the species that intervene in the reaction are lumped in order to obtain a less complex reaction scheme.

In this paper, a model that details the species involved in the mechanism into various groups, and accounts for both deactivation and poisoning, is described. The experimental results used to fit this model were already published in a previous article [43].

2. Model description

Eight lumps were accounted for in the construction of this model: reactant, cyclopentane ring isomers, alkanes, alkenes, aromatics, nitrogen compounds (in this case quinoline), coke and nitrogen containing coke. Four elementary reactions were considered: cracking (ring opening by β-scission followed by secondary cracking also by β-scission), isomerization, hydrogen transfer and aromatics condensation. In the cracking reactions it is considered that one reactant molecule reacts with the production of n molecules of alkenes. The variable n is to be seen as an average stoichiometric coefficient which was introduced to account for the existence of reactions consecutive to the initial cracking step itself, namely the oligomerization (2 alkenes → 1 heavier alkene) and oligomerization–cracking reaction pathways; in the absence of these secondary reactions the stoichiometric coefficient would be equal to 2 but, so that these side reaction are not explicitly taken into account, n is used as a model parameter. Cracking of the paraffin molecules produced by the side reactions was not explicitly considered.

2.1. Reactions

This is a pseudo-homogeneous model; all equations were obtained assuming that all reactants and products, with the exception of coke molecules and quinoline, were in the gas phase.

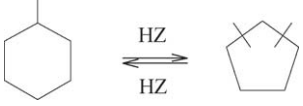

(r1)

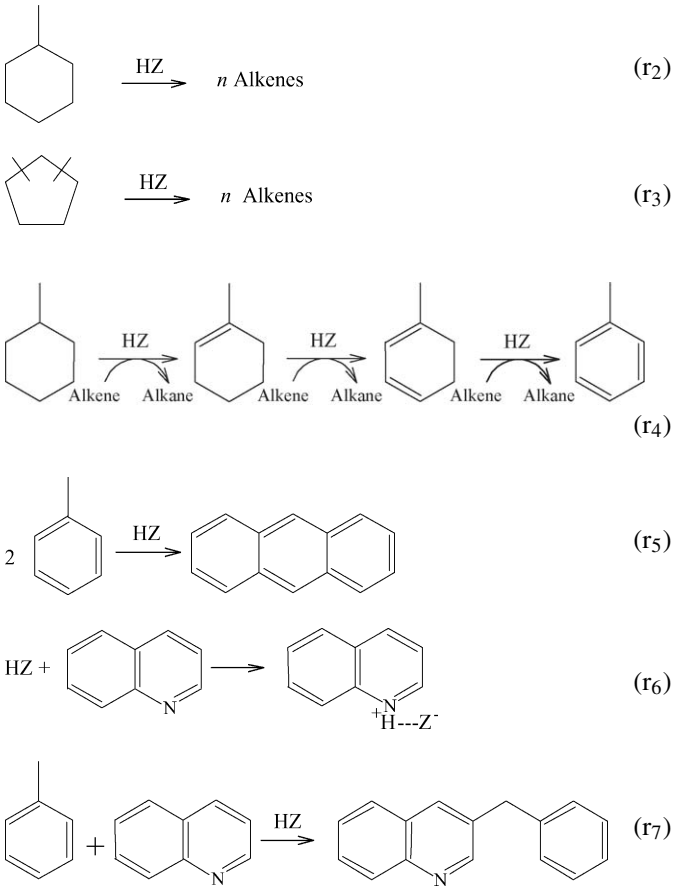

2.2. Reaction rates

The rate of each reaction in the pseudo-homogeneous phase is assumed to be described by the following expression:

$$r_k(\text{mol g}^{-1}\,\text{s}^{-1}) = k_k \prod_{i=0}^{n_k} p_i^{m_{i,k}} [\text{HZ}](1+\gamma w^2)^{-1} \quad (1)$$

where k_k is the rate constant of the reaction k, n_k the number of reactants on the reaction k, [HZ] the free Brønsted acid sites density, p_i the partial pressure of the species i, $m_{i,k}$ the molecularity of the compound i in the reaction k, w the carbon content in the zeolite and $(1+\gamma w^2)^{-1}$ is a term which accounts for diffusion limitations caused by coke [12].

For reaction (r4), the first step was assumed to be limiting due to the inexistence of intermediaries in the reactional mixture. This means that the hydrogen transfer rate was assumed to be given by $r_4 = k_4 p_{\text{mch}} p_{\text{alkenes}} [\text{HZ}](1+\gamma w^2)^{-1}$. For the coke formation reactions it was necessary to add a term which accounted for the decrease in coke formation due to the microporous volume limitations of the zeolite [12]:

$$r_k(\text{mol g}^{-1}\,\text{s}^{-1}) = k_k \prod_{i=0}^{n_k} p_i^{m_{i,k}} [\text{HZ}](1+\gamma w^2)^{-1} \left(1 - \frac{w}{w_{\max}}\right) \quad (2)$$

where $w_{\max}$ is maximum amount of coke formed in the H-USY zeolite for this reaction. It was assumed to be equal to the carbon

content in the zeolite after 4 h of reaction with methylcyclohexane alone: 8%.

2.3. Material balances

The material balance to the species in the gas phase comes as follows, assuming a CSTR reactor:

$$\frac{dn_i}{dt} = F_i^{in} - F_i + r_i W \quad (3)$$

where n_i is number of moles of the species i in the reactor, F_i^{in} the inlet molar flow of the component i, F_i the outlet molar flow of i, r_i the sum of the transformation rates (production and consumption) of the species i and W is the catalyst mass. Dividing both sides of Eq. (3) by V_R/RT, where V_R is the reactor volume, R the perfect gas constant and T is the reaction absolute temperature, the balance becomes:

$$\frac{dp_i}{dt} = \frac{Q_v}{V_R}[p_i^{in} - p_i] + \frac{r_i WRT}{V_R} \quad (4)$$

where p_i^{in} is the partial inlet pressure of the component i, p_i the outlet partial pressure of the component i and Q_v is the volumetric flow.

One drawback of this model is that it assumes the reactor to behave like a continuously stirred tank reactor (CSTR). In practice, the fixed bed reactor used in the catalytic test does not have the main characteristics of a CSTR; in fact, its geometry is closer to the one of a plug flow reactor. This is an idealized system where maximum theoretical efficiencies can be attained. In practice, however, the hydrodynamics of fixed bed reactors are between plug flow and CSTR. Deviations from ideal plug flow are due to back-mixing within the reactor, the resulting product streams having a more widespread distribution of residence times. Furthermore, under extreme hydrodynamic conditions, namely for very small L/D ratios as it is the case, when axial mixture is very high, reactor partial pressures may be assumed to be uniform within the reactor (CSTR model).

3. Experimental

3.1. Experimental data

H-USY zeolite was obtained by calcination of NH_4-USY zeolite (CBV500, supplied by PQ) under air flow at 500 °C for 12 h; its physicochemical properties are presented in Table 1.

The crystallites size was estimated by scanning electron microscopy.

Nitrogen adsorption measurements were performed at −196 °C with the gas adsorption system ASAP 2000 (Micromeritcs). The microporous volume was estimated by the *t*-plot method using the Harkins and Jura standard isotherm.

The acidity of the samples was measured by adsorption of pyridine followed by IR spectroscopy, on a Nicolet 750 MAGNA-IRTM spectrometer. The samples were compressed into very thin wafers (5–15 mg/cm^2). Prior to measurements, the wafers were pre-treated in situ at 450 °C for 12 h under air flow (60 ml min^{-1}) and then at 200 °C for 1 h under vacuum (1×10^{-8} atm). For the coked zeolites, only the last part of the treatment was performed, mainly to avoid alterations in the samples.

The chemisorption of pyridine (Sigma–Aldrich, IR spectroscopic grade) was done by contacting the sample with pyridine for 15 min at 150 °C with a large excess of the nitrogenated base. The physisorbed pyridine was removed for 1 h under vacuum at the same temperature.

The reaction was performed in a Pyrex fixed-bed reactor at 350 °C and atmospheric pressure. The reactor feed was constituted by 10 mol% of methylcyclohexane (Sigma–Aldrich, 99% pure, percolated over SiO_2 before the reaction) and 90 mol% of N_2. In the poisoning tests, 0.5 wt% (540 ppm of basic nitrogen) of quinoline (Sigma–Aldrich, 96% pure) was added to the methylcyclohexane. Before reaction, the zeolite was pre-treated at 450 °C under a nitrogen flow for 8 h. The tests were performed for two values of 1/WHSV (weight hourly space velocity): 4 and 12 min. The 1/WHSV was altered by varying the mass (100, 300 mg) of catalyst and maintaining the methylcyclohexane flow constant (2.57×10^{-2} g min^{-1}). Samples of the reactor effluent were taken for several values of time-on-stream (TOS): 1, 4, 9, 14, 29 and 59 min. The reaction products were analyzed in a VARIAN 3400 chromatographer with a Plot Al_2O_3/KCl 50 m fused silica capillary column, using a flame ionization detector.

The carbon and nitrogen contents of the coke were analyzed by total combustion at 1050 °C with a mixture flow of helium and oxygen in a Thermoquest NA2100 analyzer.

3.2. Model implementation

All the reactions considered in the present system are extremely fast with the exception of coke formation reactions which are much slower; this difference in the timescale for the various reactions makes the corresponding system

Table 1
Physicochemical properties of the H-USY zeolite

Unit cell formula	Porous volume (cm^3 g^{-1})		Crystallites size (μm)	Amount of acid sites[a] (μmol g^{-1})			
	Micro	Meso		Brønsted		Lewis	
				150 °C	350 °C	150 °C	350 °C
$Na_{0.4}H_{29.6}Al_{30}Si_{162}O_{384}$,22.7EFAL	0.288	0.061	0.5	688	426	184	84

[a] Acid sites able to retain pyridine adsorbed at 150 and 350 °C.

of differential equations stiff. The integration of these systems requires a very short step and a very large integration interval.

Two methodologies can be used to avoid a very long integration time: on one hand specific integration methods can be used (backward differentiation methods or gear methods), or, in alternative, some modifications can be introduced in the model with the objective of reducing the integration time.

One way of looking to the problem is assuming that the partial pressures of the species in the gas phase are in steady state and only the amount of coke changes with time. Therefore, one describes the global transient system as a steady state one which suffers successive perturbations, by the slower processes, which change the initial state. Consequently, during the integration of the slow reactions, i.e. coke formation, the partial pressures of the gas phase products are assumed to be the steady state values corresponding to that TOS value. The simultaneous resolution of Eqs. (1), (2) and (4) with $dp_i/dt = 0$ can be used for determining the partial pressure of each gas phase species in steady state for each value of [HZ], w and W (Appendix A).

In principle, this approximation will be valid if the steady state, for all the gas phase species, is reached much faster than the step required to do the integration of the slower reactions. In Fig. 1a one can see that the steady state (1/WHV = 4 min, V_R = 5 ml) is reached after only about 2 s. On the other hand, a much longer integration step can be used to integrate the evolution of carbon content with TOS; consequently, the simplification will provide accurate results.

This can be confirmed in Fig. 1b, the results obtained with the simplified model are very close to the ones that were determined by the complete model by integration using the *Euler* method with a very small integration step. Nonetheless, some non-negligible differences are noticeable for short TOS values, which could be limiting if experimental data was located in this interval. However, the experimental points are all located in the 60–3540 s interval, which means that the steady state approximation can be used without introducing significant errors in the results.

The dependency of [HZ] with the amount of coke in the catalyst cannot be easily described. The first difficulty is that only one model coke molecule is considered when in reality several different coke molecules are produced, each with different deactivation abilities. Besides, the H-USY acid sites do not present all the same acid strength; however, one assumes that all the sites able to retain pyridine at 150 °C are equally active in methylcyclohexane transformation. The decrease in accessible Brønsted acid sites density can be determined by pyridine adsorption followed by FTIR spectroscopy [10]. The amount of acid –OH groups can be determined by subtraction of the spectra of the –OH groups after pyridine adsorption to the spectra for the fresh zeolite. This difference spectrum (Fig. 2a) corresponds to the acid sites accessible to pyridine at 150 °C. One simplified way of expressing the decrease in acid sites with TOS is by accounting the decrease in the area of the 3700–3350 cm^{-1} region which correspond to potentially active –OH groups. The evolution of the acid sites density with carbon content is represented in Fig. 2b. One can fit an exponential trendline through

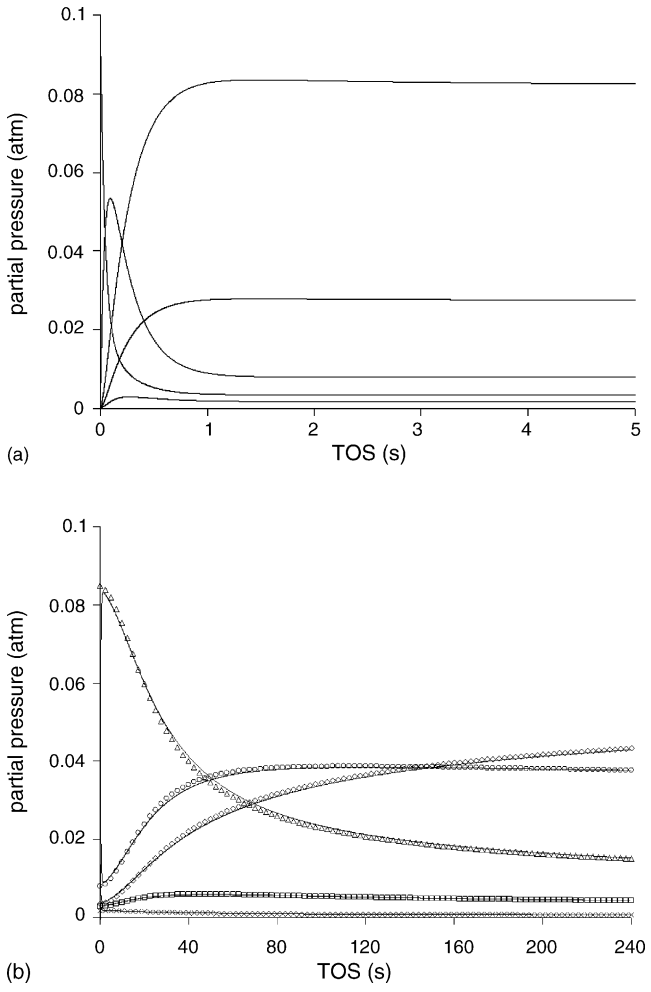

Fig. 1. (a) Partial pressures vs. TOS obtained with the complete model (constants obtained by fitting of the simplified model but with k_5 = 0; 1/WHSV = 4 min; V_R = 5 ml). (b) Comparison between the partial pressures obtained by integration of the complete model (constants obtained by fitting of the simplified model; 1/WHSV = 4 min; V_R = 5 ml) and the solution given by the simplified model (stationary state which suffer successive perturbations) for the (◊) methylcyclohexane, (◯) isomers, (△) alkanes, (□) aromatics and (×) alkenes.

the experimental data and obtain the following expression:

$$[\mathrm{HZ}](\mu\mathrm{mol\,g_{cat}^{-1}}) = 688(\mu\mathrm{mol\,g_{cat}^{-1}})\exp(-17.5 \times w(\mathrm{g_{coke}\,g_{cat}^{-1}})) \quad (5)$$

The model was fitted by minimizing the error function determined by the following expression:

$$F = \sum_{i=1}^{k} A_i \left(\frac{X_{\mathrm{exp}}^i - X_{\mathrm{model}}^i}{X_{\mathrm{exp}}^i} \right)^2 \quad (6)$$

where F is the error function, A_i the relative weight given to variable X_i, X_{exp}^i the experimental value of the variables and X_{model}^i is the value calculated by the model. The optimization was carried out by the *SOLVER*® routine in a *Microsoft Excel*® spreadsheet. Estimates for the error on the parameters were obtained by a bootstrap re-sampling technique; 10 estimates were obtained,

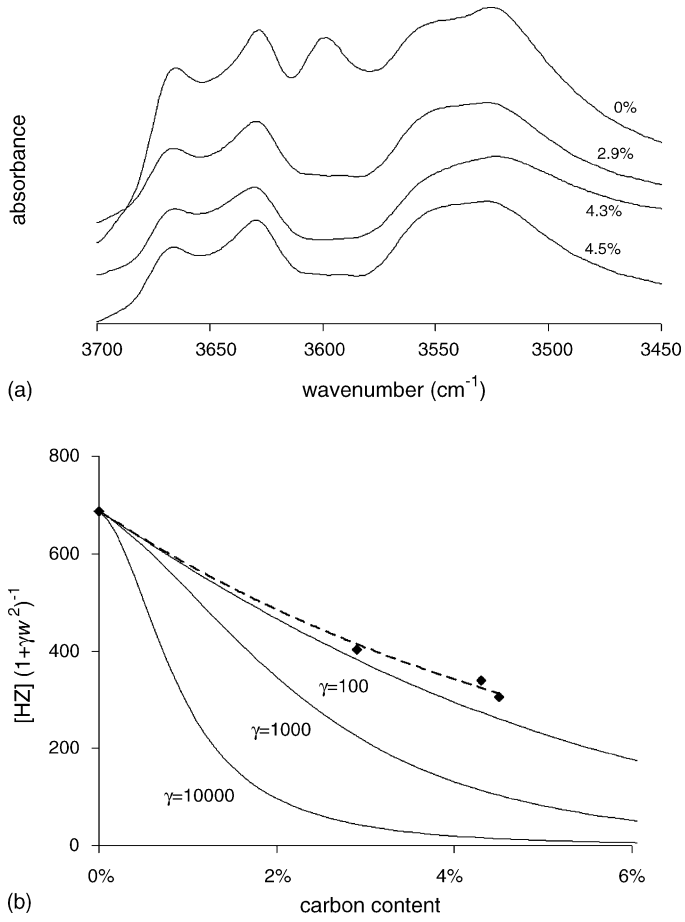

Fig. 2. (a) Potentially active ─OH groups accessible to pyridine for several carbon content values. (b) (♦) Evolution of the amount of free acid sites accessible to pyridine vs. the carbon content in the zeolite. (—) Effect of γ in the value of $[HZ](1+\gamma w^2)^{-1}$.

using a full optimization procedure for each re-sampled data set.

4. Results and discussion

The comparison between the experimental data and the fitted model are present in Fig. 3; the constants that were obtained are given in Table 2.

As it can be seen in Fig. 3a–d, the model agrees extremely well with experimental values of total conversion and yields in all three families of gas phase products: alkanes, alkenes, isomers and aromatics. The model also fits very well the experimental values of deactivation with TOS. For the tests performed without quinoline, this deactivation is due to coke formation.

On the other hand, in the poisoning tests, a large part of the deactivation with TOS is due to the almost irreversible interaction of quinoline with Brønsted acid sites. As before, the poisoning effect of quinoline is also well fitted by model. In fact, there is an increase in the poisoning effect with the decrease of 1/WHSV, mainly because the ratio of quinoline molecules per mass of zeolite is higher.

The value of n is coherent with the experimental product distribution (Fig. 4), the average carbon number of the cracking products obtained experimentally is very close to $7/n = 4.6$. However, accordingly to the β-scission mechanism, the cracking of C_7 naphtenes should produce almost exclusively non-cyclic C_7 molecules by ring opening and C_3 and i-C_4 products by secondary cracking. This would correspond to an average carbon number of exactly 3.5 ($n = 2$). In reality, products in C_5 and C_6 are also produced in non-negligible amounts. They result from oligomerization reactions between adsorbed species and alkenes, forming by this route higher molecular weight compounds that can easily crack originating products other than C_3 and C_4.

Dimethylcyclopentane isomers are among the main products of this reaction. This reaction is very fast, as it can be confirmed by the experimental results and by the value of k_1. According to the value of k_{-1}, the inverse reaction is not as likely to happen; the K_{eq} estimated by fitting for this reversible reaction is around 4.

The thermodynamic value at 350 °C can be calculated by the following expression:

$$K_{eq}(T) = e^{\overbrace{-\Delta H^0 + T\Delta S^0}^{-\Delta G_T^0}/RT} \quad (7)$$

where T is the absolute temperature (623.15 K), ΔS^0 the standard variation in entropy, ΔH^0 the standard variation in enthalpy and ΔG^0 is the standard variation in Gibbs energy during the reaction.

Considering the *cis*-1,3-dimethylcyclopentane as an example, one obtains a $\Delta H^0 = 19\ kJ\ mol^{-1}$ and a $\Delta S^0 = 23\ kJ\ mol^{-1}$ [44–47]. Therefore, according to expression (7), the equilibrium constant should be smaller than 1 (~0.4). For the other isomers, the equilibrium constant remains less than 1 due to their lower enthalpy of formation. Nonetheless, the reaction occurs quite easily over this H-USY zeolite. Actually, the Gibbs energy criteria will only be respected if the reaction occurred in one single elemental step. This is clearly not the case, since the isomerization reaction involves an adsorption step, isomerization on a Brønsted acid site, and finally, a hydrogen transfer reaction with a gas phase species. In this case the direct and reverse reaction rate constants for the overall reaction will incorporate the influence of all these steps and, thus, will not comply with the thermodynamic constraint. The possibility that the direct and reverse kinetic constants were strongly correlated, and the eventuality that the reverse rate constant could be redundant was investigated. However, the removal of the parameter k_{-1} from the model led to a poorer fit. Consequently, the two reactions must be accounted for.

The value of k_3 is much higher than the value of k_2, thus suggesting that the cracking of methylcyclohexane is less probable. This can be rationalized, if one considers the nature of the initial and final species in the ring opening step: the cracking of dimethylcyclopentane isomers is likely to involve initial and final states in which the positive charge is concentrated in tertiary and secondary carbon atoms while for methylcyclohexane cracking both the initial and final species correspond to positively charged secondary carbon atoms. Hence, the cracking of

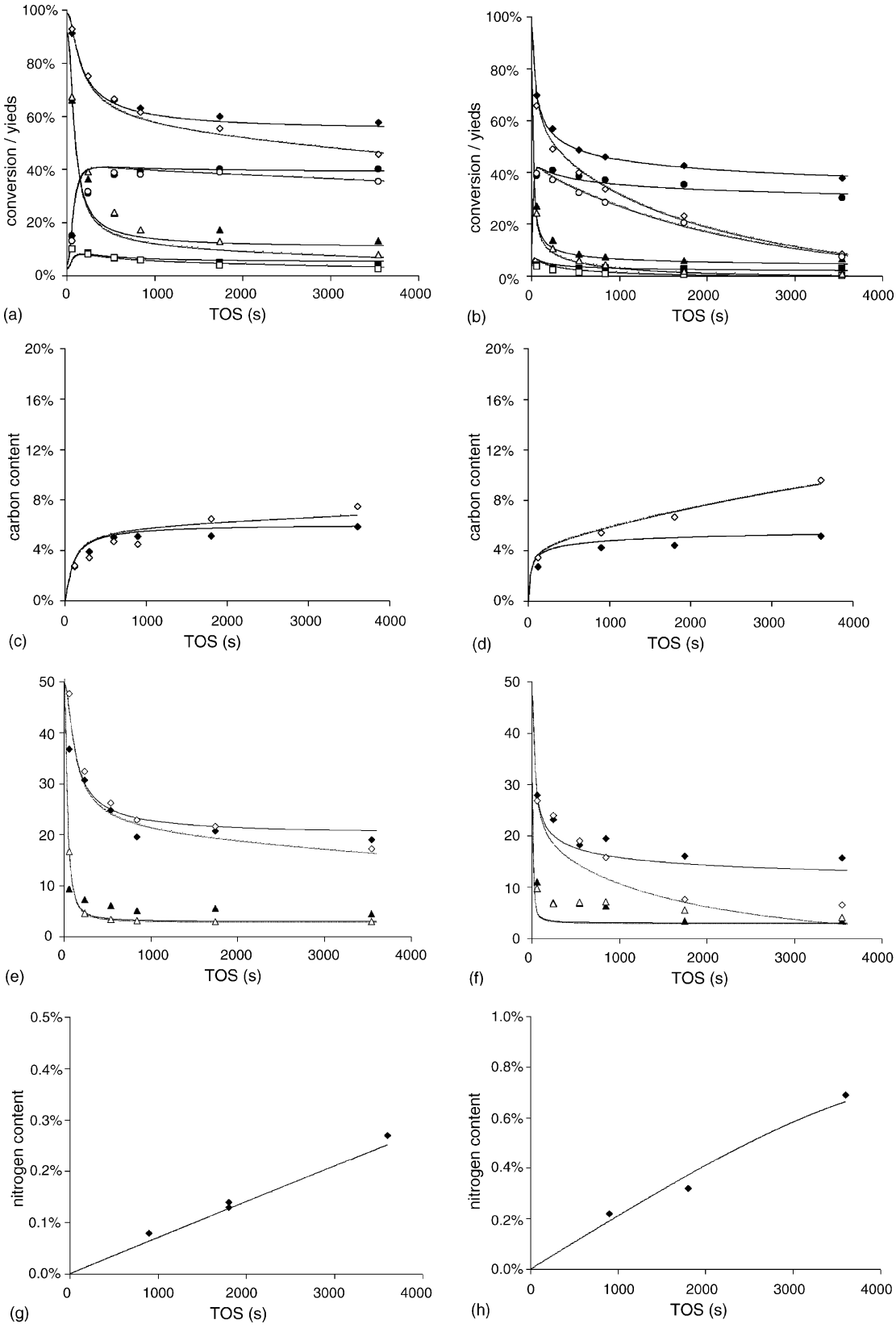

Fig. 3. (a and b) Fitting of the model, for 1/WHSV = 12 and 4 min, respectively, to the experimental values of (♦, ◊) total conversion, (●, ○) yield in isomers, (▲, △) yield in cracking products and yield in (■, □) aromatics vs. TOS. (c and d) Fitting of the model, for 1/WHSV = 12 and 4 min, respectively, to the experimental values of carbon content in the zeolite vs. TOS. (e and f) Fitting of the model, for 1/WHSV = 12 and 4 min, respectively, to the experimental values of (♦, ◊) alkanes/alkenes ratio and (▲, △) alkanes/aromatics vs. TOS. (g and h) Fitting of the model, for 1/WHSV = 12 and 4 min, respectively, to the experimental values of nitrogen content in the zeolite vs. TOS. Closed symbols, tests carried out with methylcyclohexane alone; open symbols, tests carried out with methylcyclohexane +0.5% of quinoline.

Table 2
Constants corresponding to the better fit of the experimental results for the transformation of methylcyclohexane at 350 °C over an H-USY zeolite with the model described in the text

Constant (units)	Value[a]
k_1 (atm^{-1} s^{-1})	$1.7 \times 10^2 \pm 3.1 \times 10^1$
k_{-1} (atm^{-1} s^{-1})	$3.9 \times 10^1 \pm 1.6 \times 10^1$
k_2 (atm^{-1} s^{-1})	$7.3 \times 10^0 \pm 2.9 \times 10^0$
k_3 (atm^{-1} s^{-1})	$2.8 \times 10^1 \pm 5.8 \times 10^0$
k_4 (atm^{-1} s^{-1})	$1.1 \times 10^4 \pm 3.0 \times 10^3$
k_5 (atm^{-1} s^{-1})	$3.3 \times 10^3 \pm 7.8 \times 10^2$
k_6 (atm^{-1} s^{-1})	$4.1 \times 10^2 \pm 1.3 \times 10^2$
k_7 (atm^{-1} s^{-1})	$5.2 \times 10^6 \pm 4.7 \times 10^6$
γ	$5.5 \times 10^4 \pm 7.0 \times 10^3$
n	$1.5 \times 10^0 \pm 3.4 \times 10^{-2}$

[a] The errors shown correspond to the statistical 95% confidence intervals obtained by the Bootstrap method.

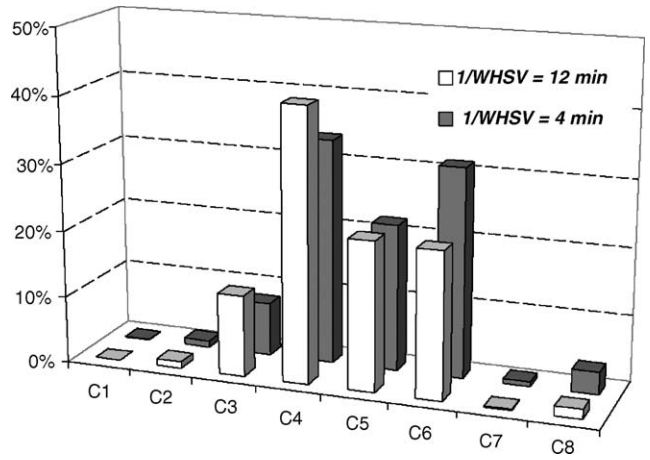

Fig. 4. Carbon number distribution of the cracking products.

isomers should be much easier and faster. Analyzing the evolution of yields with conversion (Fig. 5) one can see that the isomers have the typical behavior of an intermediary product whereas cracking is mainly a secondary reaction. Consequently,

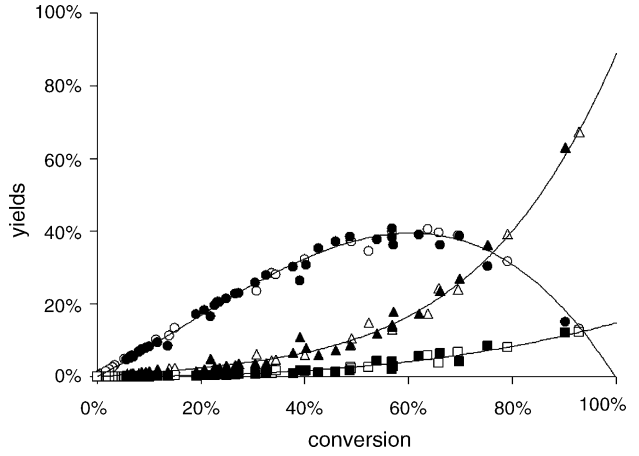

Fig. 5. Experimental yields in (●, ○) isomers, (▲, △) cracking products and (■, □) aromatics vs. total conversion. Closed symbols, tests carried out with methylcyclohexane alone; open symbols, tests carried out with methylcyclohexane +0.5% of quinoline.

the production of C_2–C_7 alkanes and alkenes occurs essentially by cracking of isomers.

A critical aspect in the transformation of hydrocarbons in acid catalysts is the existence of hydrogen transfer reactions (r_4); in the transformation of naphtenes, this importance is even higher. These reactions are extremely fast, as it can be confirmed by the value of k_4. Normally, and according to the usual β-scission mechanism, the cracking of methylcyclohexane should produce almost exclusively dimethylcyclopentane isomers and alkenes. However, the experimental values indicate that the amount of alkanes produced by hydrogen transfer is very large, many times larger than the amount of alkenes. This means that a great part of the produced alkenes suffer hydrogen transfer reactions to produce alkanes.

Both alkenes and aromatics undergo coke formation reactions:

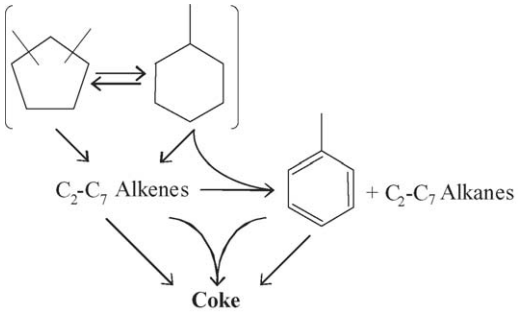

Nonetheless, the model that is presented does not account for this reaction. Analyzing the experimental data one can evaluate the importance of the role played by alkenes in coke formation. As an example, for 1/WHSV = 12 min, the mass of alkenes produced by β-scission cracking between TOS = 2 and 5 min is close to 38 mg. On the other hand, the amount of alkanes formed by hydrogen transfer reactions corresponds to about 37 mg whereas in meantime, the amount of coke deposed in the zeolite is close to 9 mg. Consequently, almost all alkenes undergo hydrogen transfer reactions and not coke formation. Moreover, this means that the formation of aromatics via alkenes cyclization is also likely to be limited.

Furthermore, from the amount of alkanes that is converted, 18 mg of aromatics should be produced; however, only 9.5 mg are detected in the TOS = 2–5 min interval. Therefore, all results seem to point to coke being mainly produced by aromatics transformation. In fact, if alkenes participated extensively in coke formation, the coke content values, aromatics yield, alkanes/alkanes and alkanes/aromatics ratios could not be fitted simultaneously by this model.

Besides the observed good agreements between the experimental data and the fitted model for the gas phase product distribution, the experimental values of the amounts of deposited carbon and nitrogen are also well correlated by the model (Fig. 3e and f). It is visible that coke forms rapidly in first few minutes of the reaction (high value of k_5) but its production decreases rapidly when the carbon content reaches values close to w_{max}.

When quinoline is added, there is an augmentation in the amount of carbon deposited in the zeolite, mainly due to retention of quinoline itself. This retention, besides decreasing the amount of available acid sites, increases diffusion limitations.

It is clear that quinoline has a great affinity towards the catalyst because the major part of the injected quinoline is retained by the zeolite for these two values of 1/WHSV (Fig. 3g and h). This explains the high value for the fitted adsorption constant k_6. Therefore, assuming an irreversible interaction of the basic nitrogen molecule with Brønsted acid sites is quite accurate.

The kinetic constant for the formation of coke from quinoline (k_7) is also very high which seems to point out that quinoline intervenes directly in coke formation. GC–MS coupling analysis confirmed this fact as it was already reported in a previous published work [42].

The diffusion limitations seem to play a very important role in deactivation. The high value of γ clearly indicates this fact.

5. Conclusions

If one considers the simplicity of the model the results that are obtained are quite good. For the tests carried out with methylcyclohexane alone, the values that are fitted for total conversion and yields are quite accurate, so are those of the alkanes/alkenes ratio and alkanes/aromatics ratio. In what concerns the amount of carbon in the catalyst, the results are also good for both contact times. The obtained set of constants leads to good results for two very different values of 1/WHSV: 12 and 4 min.

For the tests performed with quinoline the fitting is also good, the correlation between the experimental values of activity decrease caused by the base and the model is very reasonable. Besides, the experimental values of yields, alkanes/alkenes ratio, alkanes/aromatics ratio, carbon content and nitrogen content in the zeolite are also satisfactorily fitted.

The transformation of hydrocarbons, namely naphtenes, over acid catalysts at moderate to high temperatures occurs extremely quickly. The contact time necessary to obtain good conversions is very small, as it can confirmed by the 3–5 s contact time in industrial riser reactors. This implies that steady state is also reached extremely fast, which allows a rather useful simplification in the model: all the reactions, with the exception of coke formation (slower), were assumed to be in steady state.

The importance of this model relies mainly in its capacity of forecasting the deactivation with TOS as direct consequence of coke formation and poisoning. During the construction of this model it was clearly shown that accounting the coke formation reactions is essential to obtain a model which describes accurately the transformation of hydrocarbons over acid zeolites. In fact, a model without coke formation will not be able to predict simultaneously the amount of alkanes, alkenes and aromatics that are produced. The amount of aromatics consumed in coke formation cannot, in any circumstances, be neglected; mainly when the carbon content in the zeolite is high, as it is the case for FCC catalysts.

Acknowledgments

The first author expresses his gratitude to the Fundação para a Ciência e Tecnologia (FCT) for its Ph.D. grant (ref. SFRH/BD/13411/2003). Besides, all authors thank the Fundação para a Ciência e Tecnologia (FCT) for financing the project ref. POCI/EQU/58550/2004.

Appendix A. Steady state equations

In this appendix we present the derivation of the expressions for the partial pressure of species involved under the quasi-steady state approach.

$$p_{\mathrm{mch}} = \frac{-a_1 - \sqrt{{a_1}^2 - 4a_2a_0}}{2a_2} \tag{A.1}$$

$$a_2 = -3k_4\left(k_1 + k_2 + \frac{K}{[\mathrm{HZ}]}\right) + \frac{3k_4k_1k_{-1}}{\left(\frac{K}{[\mathrm{HZ}]} + k_{-1} + k_3\right)} - \left(nk_2k_4 + \frac{nk_3k_1k_4}{\left(\frac{K}{[\mathrm{HZ}]} + k_{-1} + k_3\right)}\right)$$

$$a_1 = 3k_4\frac{K}{[\mathrm{HZ}]}p_{\mathrm{mch}}^{\mathrm{in}} - \left(k_1 + k_2 + \frac{K}{[\mathrm{HZ}]}\right)\frac{K}{[\mathrm{HZ}]} + \frac{k_{-1}k_1}{\left(\frac{K}{[\mathrm{HZ}]} + k_{-1} + k_3\right)}\frac{K}{[\mathrm{HZ}]}$$

$$a_0 = \frac{K}{[\mathrm{HZ}]}p_{\mathrm{mch}}^{\mathrm{in}}$$

$$p_{\mathrm{isom}} = \frac{k_1 p_{\mathrm{mch}}}{\left(\frac{K}{[\mathrm{HZ}]} + k_{-1} + k_3\right)} \tag{A.2}$$

$$p_{\mathrm{olef}} = \frac{nk_2 p_{\mathrm{mch}} + \frac{nk_3k_1p_{\mathrm{mch}}}{\left(\frac{K}{[\mathrm{HZ}]} + k_{-1} + k_3\right)}}{\left(\frac{K}{[\mathrm{HZ}]} + 3k_4 p_{\mathrm{mch}}\right)} \tag{A.3}$$

$$p_{\mathrm{paraf}} = \frac{3nk_2k_4p_{\mathrm{mch}}^2 + \frac{3nk_4k_3k_1p_{\mathrm{mch}}^2}{\left(\frac{K}{[\mathrm{HZ}]} + k_{-1} + k_3\right)}}{\left(\frac{K^2}{[\mathrm{HZ}]^2} + \frac{3k_4p_{\mathrm{mch}}K}{[HZ]}\right)} \tag{A.4}$$

$$b_3 p_{\mathrm{aro}}^3 + b_2 p_{\mathrm{aro}}^2 + b_1 p_{\mathrm{aro}} + b_0 = 0 \tag{A.5}$$

$$b_3 = -2k_5k_7\left(1 - \frac{w}{w_{\max}}\right)^2$$

$$b_2 = -k_7\frac{K}{[\mathrm{HZ}]}\left(1 - \frac{w}{w_{\max}}\right) - 2k_5\left(1 - \frac{w}{w_{\max}}\right)\left(\frac{K}{[\mathrm{HZ}]} + k_6\right)$$

$$b_1 = -\frac{K}{[\mathrm{HZ}]}\left(k_6 + \frac{K}{[\mathrm{HZ}]}\right) - k_7\left(1 - \frac{w}{w_{\max}}\right) \times \left(p^{\mathrm{in}}_{\mathrm{quino}} + \frac{nk_2k_4p^2_{\mathrm{mch}} + \frac{nk_4k_3k_1p^2_{\mathrm{mch}}}{\left(\frac{K}{[\mathrm{HZ}]}+k_{-1}+k_3\right)}}{\left(\frac{K}{[\mathrm{HZ}]} + 3k_4p_{\mathrm{mch}}\right)}\right)$$

$$b_0 = \frac{nk_2k_4p^2_{\mathrm{mch}} + \frac{nk_4k_3k_1p^2_{\mathrm{mch}}}{\left(\frac{K}{[\mathrm{HZ}]}+k_{-1}+k_3\right)}}{\left(\frac{K}{[\mathrm{HZ}]} + 3k_4p_{\mathrm{mch}}\right)}\left(\frac{K}{[\mathrm{HZ}]} + k_6\right)$$

$$p_{\mathrm{quino}} = \frac{p^{\mathrm{in}}_{\mathrm{quino}}}{\left(\frac{K}{[\mathrm{HZ}]} + k_6 + k_7 \times p_{\mathrm{aro}}\left(1 - \frac{w}{w_{\max}}\right)\right)} \quad (A.6)$$

$$K = \frac{Q_{\mathrm{v}}}{WRT(1+\gamma w^2)} \quad (A.7)$$

References

[1] T.F. Degnan, Top. Catal. 13 (2000) 349.
[2] S. Chena, G. Manos, Catal. Lett. 96 (2004) 195.
[3] H.S. Cerqueira, C. Sievers, G. Joly, P. Magnoux, J.A. Lercher, Ind. Eng. Chem. Res. 44 (2005) 2069.
[4] P.C. Mihindou-Koumba, H.S. Cerqueira, P. Magnoux, M. Guisnet, Ind. Eng. Chem. Res. 40 (2001) 1042.
[5] H.S. Cerqueira, P. Ayrault, J. Datka, P. Magnoux, M. Guisnet, J. Catal. 196 (2000) 149.
[6] H.S. Cerqueira, P. Magnoux, D. Martin, M. Guisnet, Appl. Catal. A: Gen. 208 (2001) 359.
[7] P. Magnoux, H.S. Cerqueira, M. Guisnet, Appl. Catal. A: Gen. 235 (2002) 93.
[8] C.E. Snape, B.J. McGhee, J.M. Andresen, R. Hughes, C.L. Koon, G. Hutchings, Appl. Catal. A: Gen. 129 (1995) 125.
[9] H.S. Cerqueira, A. Rabeharitsara, P. Ayrault, J. Datka, P. Magnoux, M. Guisnet, Catalyst deactivation, in: Proceedings Studies in Surface Science and Catalysis, 139, 2001.
[10] H.S. Cerqueira, P. Ayrault, J. Datka, M. Guisnet, Microporous Mesoporous Mater. 38 (2000) 197.
[11] L.D.T. Câmara, H.S. Cerqueira, D.A.G. Aranda, K. Rajagopal, Catal. Today 98 (2004) 309.
[12] J.M. Lopes, F. Lemos, F. Ramôa Ribeiro, E.G. Derouane, P. Magnoux, M. Guisnet, Appl. Catal. A: Gen. 114 (1994) 161.
[13] A. Corma, A.L. Agudo, React. Kinet. Catal. Lett. 16 (1981) 253.
[14] W.-C. Cheng, K. Rajagopalan, J. Catal. 119 (1989) 354.
[15] A. Corma, F.A. Mocholí, Appl. Catal. 67 (1990) 307.
[16] G. de la Puente, U. Sedran, Appl. Catal. A: Gen. 144 (1996) 147.
[17] E. Falabella Sousa-Aguiar, C.J.A. Mota, M.L. Murta Valle, M. Pinhel da Silva, D. Forte da Silva, J. Mol. Catal. A: Chem. 104 (1996) 267.
[18] H.S. Cerqueira, P.C. Mihindou-Koumba, P. Magnoux, M. Guisnet, Ind. Eng. Chem. Res. 126 (2001) 1050.
[19] W.O. Haag, R.M. Dessau, 8th International Congress of Catalysis, II, 1984, p. 305.
[20] A. Corma, J. Planelles, J. Sánchez-Marín, F. Tomás, J. Mol. Catal. A: Chem. 32 (1985) 365.
[21] J.A. van Bokhoven, B.A. Williams, W. Ji, Diek C. Koningsbergerc, H.H. Kung, J.T. Miller, J. Catal. 224 (2004) 50.
[22] F.C. Whitmore, Ind. Eng. Chem. (1934) 94.
[23] B.S. Greensfelder, H.H. Voge, G.M. Good, Ind. Eng. Chem. 41 (1949) 2573.
[24] A. Corma, A.V. Orchillés, Microporous Mesoporous Mater. 35–36 (2000) 21.
[25] R. Ramos Pinto, P. Borges, M.A.N.D.A. Lemos, F. Lemos, F. Ramôa Ribeiro, Appl. Catal. A: Gen. 272 (2004) 23.
[26] D.L. Liguras, D.T. Allen, Ind. Eng. Chem. Res. 28 (1989) 674.
[27] M.A. Baltanas, K.K. Van Raemdonck, G.F. Froment, R.S. Mohedas, Ind. Eng. Chem. Res. 28 (1989) 899.
[28] W. Suarez, W.-C. Cheng, K. Rajagopalan, A.W. Peters, Chem. Eng. Sci. 45 (1990) 2581.
[29] N.V. Dewachtere, F. Santaella, G.F. Froment, Chem. Eng. Sci. 54 (1999) 3653.
[30] A. Corma, F.V. Melo, L. Sauvanaud, Appl. Catal. A: Gen. 287 (2005) 34.
[31] T.M. Moustafa, G.F. Froment, Ind. Eng. Chem. Res. 42 (2003) 14.
[32] G. Yaluris, J.E. Rekoske, L.M. Aparicio, R.J. Madon, J.A. Dumesic, J. Catal. 153 (1995) 54.
[33] G. Yaluris, J.E. Rekoske, L.M. Aparicio, R.J. Madon, J.A. Dumesic, J. Catal. 153 (1995) 65.
[34] M.A. Sanchez-Castillo, N. Agarwal, C. Miller, R.D. Cortright, R.J. Madon, J.A. Dumesic, J. Catal. 205 (2002) 67.
[35] M.A. Sanchez-Castillo, N. Agarwal, A. Bartsch, R.D. Cortright, R.J. Madon, J.A. Dumesic, J. Catal. 218 (2003) 88.
[36] G. Yaluris, R.J. Madon, J.A. Dumesic, J. Catal. 165 (1997) 205.
[37] C.I.C. Pinheiro, F. Lemos, F. Ramôa Ribeiro, Chem. Eng. Sci. 54 (1999) 1735.
[38] H. Carabineiro, C.I.C. Pinheiro, F. Lemos, F. Ramôa Ribeiro, Chem. Eng. Sci. 59 (2004) 1221.
[39] G. Yaluris, R.J. Madon, J.A. Dumesic, J. Catal. 186 (1999) 134.
[40] A. Monzon, E. Romeo, A. Borgna, Chem. Eng. J. 94 (2003) 19.
[41] H.S. Cerqueira, P. Magnoux, D. Martin, M. Guisnet, in: 216th ACS Meeting, FUEL Division - Symposium on Reactor and Reaction Modeling, 43, 1998, p. 626.
[42] P. Borges, R. Ramos Pinto, M.A.N.D.A. Lemos, F. Lemos, J.C. Védrine, E.G. Derouane, F. Ramôa Ribeiro, J. Mol. Catal. A: Gen. 229 (1–2) (2005) 127.
[43] G. Caeiro, P. Magnoux, J.M. Lopes, F. Ramôa Ribeiro, Appl. Catal. A: Gen. 292 (2005) 189.
[44] C.W. Beckett, J. Am. Chem. Soc. 69 (1947) 2488.
[45] E.J. Prosen, W.H. Johnson, F.D. Rossini, J. Res. NBS 37 (1946) 51.
[46] W.H. Johnson, E.J. Prosen, F.D. Rossini, J. Res. NBS 42 (1949) 251.
[47] D.R. Stull, The Chemical Thermodynamics of Organic Compounds, Wiley, New York, 1969.